Indian monsoon's relation with the decadal part of PDO in observations and NCAR CCSM4

Running Title: Relation between Indian monsoon & decadal PDO in observations & CCSM4

Lakshmi Krishnamurthy[1] and V. Krishnamurthy[2]

[1]*Department of Atmospheric, Oceanic and Earth Sciences*

George Mason University, Fairfax, Virginia

[2]*Center for Ocean-Land-Atmosphere Studies*

George Mason University, Fairfax, Virginia

Initial Submission: June 2015

Revision: November 2015

Revision: April 2016

Revision: May 2016

Corresponding author's address:

Lakshmi Krishnamurthy

NOAA Geophysical Fluid Dynamics Laboratory

Princeton University Forrestal Campus

201 Forrestal Road

Princeton, NJ 08540-6649

Lakshmi.Krishnamurthy@noaa.gov

Abstract

This study has investigated the influence of the decadal component of the Pacific Decadal Oscillation (PDO) on the Indian monsoon in observations and coupled climate model. A major part of the conventionally defined PDO is shown to be dominated by interannual variability. By extracting the pure decadal part of the North Pacific variability, this study has shown that the Indian monsoon rainfall exhibits different relations with the conventionally defined PDO and the pure decadal component of the PDO. This result may have implications for decadal prediction of the monsoon. The analysis suggests that the warm (cold) phase of pure decadal variability of PDO is associated with deficit (excess) rainfall over the west central part of India. In contrast, the conventional warm (cold) PDO index is associated with deficit (excess) rainfall over most of India. The warm phase of the pure decadal PDO opposes the moisture flow beyond 20°N over the Indian monsoon region via the meridional winds extending from the North Pacific and leads to reduced rainfall over west central India. The Community Climate System Model Version 4 (CCSM4) of the National Center for Atmospheric Research shows reasonable simulation of the decadal PDO mode in both the North Pacific sea surface temperature and the Indian monsoon rainfall and the relation between them. Further, the observed and simulated PDO-monsoon relation is substantiated through a regionally de-coupled experiment. The coupled model experiment also provides supporting evidence for the mechanism involving the intermediary role played by the tropical Pacific Ocean in the PDO-monsoon relation.

Keywords: PDO, Indian monsoon, decadal, CCSM4, North Pacific, Tropical Pacific

1 Introduction

The Indian monsoon is a prominent component of the global climate system and contributes significantly to the climate variability. Climate change is known to have considerable influence on the variability of the Indian monsoon at various time scales (e.g., Turner and Annamalai, 2012). In addition to the anthropogenic effects, natural variability on interannual and decadal timescales is also considered the integral part of the climate change. Since the Indian monsoon affects the lives of millions of people, it is important to understand the factors which determine the climate change over India. On interannual timescale, El Niño-Southern Oscillation (ENSO) is known to have a major impact on the Indian monsoon (Sikka, 1980; Rasmusson and Carpenter, 1983). The ENSO is also shown to play a role in the Indian monsoon variability on interdecadal timescale (Krishnamurthy and Goswami, 2000; Krishnan and Sugi, 2003). On decadal to multidecadal timescales, the Pacific Decadal Oscillation (PDO), the Atlantic Multidecadal Oscillation (AMO) and the Atlantic tripole mode determine the variability of rainfall over India (Zhang and Delworth, 2006; Lu et al., 2006; Li et al., 2008; Sen Roy, 2011; Sen Roy et al., 2003; Krishnamurthy and Krishnamurthy, 2014a, 2014b, 2016b).

Some studies (Sen Roy, 2011; Krishnamurthy and Krishnamurthy, 2014a) have explored the relation between the PDO in observations and coupled climate model. Krishnamurthy and Krishnamurthy (2014a) analyzed observations and simulations from the Community Climate System Model Version 4 (CCSM4) of National Center for

Atmospheric Research (NCAR) and showed that there is significant correlation between PDO and Indian monsoon rainfall with the warm (cold) phase of PDO associated with below-normal (above-normal) conditions over India. The PDO was also shown to modulate the ENSO-monsoon relationship. When ENSO and PDO are in (out of) phase, they enhance (counteract) the ENSO-monsoon relation. The mechanism for the PDO-monsoon relation was also suggested through the Walker and Hadley circulations with the tropical Pacific playing an intermediary role between the North Pacific and the Indian monsoon. The coupled model, CCSM4 was shown to successfully simulate the observed PDO-monsoon relation, decadal modulation of the ENSO-monsoon relation and the mechanism.

However, the earlier studies (Sen Roy, 2011; Krishnamurthy and Krishnamurthy, 2014a) have used the conventional definition of PDO index based on the EOF analysis of detrended monthly sea surface temperature (SST) anomalies over the North Pacific (120°E–120°W, 20°N–60°N). This index consists of both the interannual and decadal components of the North Pacific variability. The study of the relation between the PDO and the Indian monsoon using this index would include the effects of the interannual and decadal PDO on the Indian monsoon but not the impact of the pure decadal part of the PDO. Thus, when we refer to the teleconnections of the decadal variability of the North Pacific, it is important to isolate the pure decadal variability associated with the North Pacific to understand its relation with the Indian monsoon.

This study makes use of a data-adaptive method to extract the pure decadal component of PDO to understand its teleconnection with the Indian monsoon. This study is an extension of Krishnamurthy and Krishnamurthy (2014a) and has three objectives. The first objective is to understand the differences in the influence of the decadal plus interannual component and the pure-decadal component of PDO on the observed Indian monsoon variability. We make use of the results of Krishnamurthy and Krishnamurthy (2014b) who have documented the PDO-related pure decadal modes in the Indian rainfall and the North Pacific SST. The second objective is to demonstrate the ability of the coupled climate model CCSM4 to simulate the PDO-related pure decadal components of variability in the Indian monsoon rainfall and the North Pacific SST, and the decadal PDO-monsoon relation. The third objective is to substantiate the observed and model simulated PDO-monsoon relation through the regionally de-coupled model experiment with CCSM4. The relation between the North Pacific and the tropical Pacific variability is compared between the control and experimental runs to provide evidence for the mechanism suggested by Krishnamurthy and Krishnamurthy (2014a).

The observed data, model control simulation and experiment, and the method of analysis are discussed in section 2. The differences between the relations of the interannual plus decadal PDO and the pure decadal PDO with the Indian monsoon in the observations are explored in section 3. The PDO-related decadal modes in the Indian rainfall and the North Pacific SST, and the relation between them in the model

simulations are presented in section 4. Section 5 discusses the role of the tropical Pacific in the PDO-monsoon relation. The results are summarized in section 6.

2 Data, model and method of analysis

2.1 Observed data

The monthly mean SST data set HadISST1.1, based on optimal interpolation procedure, from the Hadley Centre for Climate Prediction and Research for the period 1870–2006 (Rayner et al., 2003) is used. This study uses two rainfall data sets. The first rainfall data set is from the India Meteorological Department (IMD) which is on 1° longitude × 1° latitude grid and was constructed from daily rain gauge observations from more than 2000 stations distributed over India (Rajeevan et al., 2008). It spans the period 1901–2004, and the data coverage is only over the land region of India. The second data set is from Smith et al., (2010) which is based on merged statistical analyses of monthly precipitation anomalies. This data set is on 5° longitude × 5° latitude grid for the period 1900-2008. It has global coverage over both land and oceanic regions. The Twentieth Century Reanalysis version 2 (20CR2) from the National Oceanic and Atmospheric Administration–Cooperative Institute for Research in Environmental Sciences (NOAA-CIRES) provided the zonal and meridional winds at 19 vertical levels (1000–100 hPa) with a horizontal resolution of 2° longitude × 2° latitude for the period 1871–2008 (Compo et al., 2011).

2.2 Model control simulation and experiment

This study uses the data from the control simulation of CCSM4 obtained from NCAR. The details of CCSM4 are provided in Gent et al., (2011). The control simulation in this study is the 20th Century Climate in Coupled Models (20C3M) simulation by CCSM4 which was run from January 1850 to December 2005. This control run will be referred to as CTL hereafter. This coupled model has atmosphere and land components at 2° horizontal resolution and ocean component at 1° horizontal resolution. The initial conditions for this simulation were obtained from the pre-industrial run.

To provide support to the PDO-monsoon relation showed by Krishnamurthy and Krishnamurthy (2014a), we have performed a de-coupled model experiment. The methodology suggested in Huang (2004) and Huang et al. (2004) is employed for this experiment. In this experiment, the monthly climatological mean SST (this annual cycle repeats every year) from the 20C3M control run is prescribed in the North Pacific region (20°N–60°N in latitude and from west coast to east coast in longitude). Thus, the atmosphere feels the climatological SST in this domain rather than the model generated SST. The rest of the oceanic basins are fully coupled wherein the atmosphere feels the SST generated by the ocean model. A 10° buffer zone was used between the coupled and uncoupled regions. The initial conditions are based on same conditions used for 20C3M control run, thus ensuring that the model does not have any spin-up issues. This experiment was also run from January 1850 to December 2005. The experimental run

will be referred to as EXP hereafter. The results from this experiment have been thoroughly investigated for any model drift issues. This experiment is also successfully used to demonstrate the effect of the North Pacific on the Indian Ocean SST (Krishnamurthy and Krishnamurthy, 2016a).

2.3 Method of analysis

This study employs multi-channel singular spectrum analysis (MSSA; Ghil et al., 2002) to extract the decadal signal in the North Pacific. This method is the multivariate version of the singular spectrum analysis (SSA; Broomhead and King, 1986). Given a time series $X(t)$ at L grid points (channels) and time $t = 1, 2, 3 \ldots N$, a lagged covariance matrix C is constructed by supplementing the time series with M lagged copies. A diagonalization of the matrix C yields LM eigenvalues and LM eigenvectors. The eigenvectors are the space-time empirical orthogonal functions (ST-EOFs). The space-time principal components (ST-PCs) are obtained by projecting the original times series $X(t)$ onto the corresponding ST-EOFs. The ST-EOF and ST-PC of each eigenmode is suitably combined (see Ghil et al., 2002 for the formula) to obtain the corresponding reconstructed component (RC) which has the same spatial and temporal dimensions as the original time series and also captures its phase. A pair of eigenmodes is identified to be oscillatory if the eigenvalues are nearly degenerate, the ST-EOFs and ST-PCs are in quadrature and the periods are nearly equal (Plaut and Vautard, 1994). When a single time series is considered ($L = 1$ case), the method is referred as SSA. The details and

application of the method are provided by Ghil et al., (2002) and Krishnamurthy and Krishnamurthy, (2014b).

The statistical significance of the MSSA eigenmodes is determined by using the Monte-Carlo MSSA test described by Allen and Robertson (1996), Allen and Smith (1996) and Krishnamurthy and Krishnamurthy (2014b). All the MSSA and SSA eigenmodes discussed in this paper satisfy 5% significance level. This technique has been successfully applied on the observed Indian monsoon rainfall and the North Pacific, North Atlantic and Indian Ocean SST in Krishnamurthy and Krishnamurthy (2014b, 2016a, 2016b).

Further analyses in this study consist of correlations and regressions for which the statistical significance was found by *t*-test. The degrees of freedom in calculating the confidence interval for *t*-test is determined based on the *e*-folding time of the autocorrelation function of the decadal mode (e.g., Leith 1973). This takes into account the persistent nature of the decadal modes. The 5% significance level for the spectra of time series is computed with respect to the spectrum of the corresponding red noise. In this study, we also use stationary moisture flux at JJAS seasonal mean time scale (see, for example, Dominguez and Kumar 2005 for the formula). We make use of JJAS seasonal means from 20th century reanalysis data from NOAA-CIRES to calculate the moisture flux. Here, stationary refers to seasonal mean.

3 Decadal component of PDO in observation

The PDO is conventionally defined from an EOF analysis of the SST anomalies over the North Pacific Ocean, following Mantua et al. (1997). The PDO is extracted by performing an EOF analysis of detrended monthly SST anomalies in the region (120°E–120°W, 20°N–60°N) for the period 1870–2006. The first PC (PC1), shown in Fig. 1a, has been defined as the conventional PDO index. The corresponding first EOF (EOF1) and PC1 are discussed in more detail by Krishnamurthy and Krishnamurthy (2014a). The noticeable feature of the PDO index (Fig. 1a) is the strong presence of the interannual variability along with the decadal-scale variability. Thus, the relation between this PDO index and the Indian monsoon, as discussed by Krishnamurthy and Krishnamurthy (2014a), includes the influence of both the interannual and decadal components of the PDO (and hence also referred to as the total PDO index in this paper).

To better understand the teleconnection of the decadal variability of the North Pacific with the Indian monsoon, it is necessary to extract the pure decadal signal of the PDO, i.e., without the presence of the interannual fluctuation in the North Pacific SST. This can be achieved by applying SSA on the conventional total PDO index shown in Fig. 1a. As described in section 2.3, SSA is applied on a single variable time series and can extract oscillatory modes. The SSA was applied on the conventional total PDO index, presented in Fig. 1a, using a lag window of 720 months for the period 1870–2006. The eigenmodes from the SSA which emerge as the oscillatory pairs with the decadal time scale of the PDO were identified, and the RC of the decadal oscillation was constructed

(see Ghil et al., 2012 for the method to construct the RC). The time series of the RC, shown Fig. 1b, reveals decadal scale variability without the presence of interannual fluctuations. The time period of this oscillation, determined from power spectrum analysis, indicates a peak centered at 20 years (Fig. 1c). The RC presented in Fig. 1b will be referred to as the PDO-Decadal (PDO-D) index. The regression of June-September (JJAS) seasonal anomalies of SST on JJAS mean PDO-D index captures negative anomalies in the central Pacific surrounded by positive anomalies extending along the coast of North America to the eastern equatorial Pacific (Fig. 2a), the typical signature of the warm phase of PDO.

Further regression analysis is carried out to determine the relation with precipitation and circulation. The regression of JJAS seasonal anomalies of precipitation (from Smith et al., 2010 data) on the JJAS mean PDO-D index is shown in Fig. 2b. The precipitation regression pattern captures the tripole signature of rainfall associated with the Walker circulation with positive anomalies in the equatorial Pacific and Indian Ocean along with negative anomalies around the Maritime Continent. The negative rainfall anomalies over India indicate the drought condition (Fig. 2b) associated with the warm phase of PDO (Fig. 2a).

While the regression in Fig. 2b shows the precipitation pattern over land and oceanic regions, it does not provide a detailed structure over India because of the coarse resolution of the Smith et al., (2010) precipitation data. This shortcoming is resolved by using the higher resolution precipitation data from IMD but with coverage only over

India. The rainfall regression pattern using the IMD data also indicates drought condition over a large part of central India (Fig. 3a) along with regions of above-normal condition. Thus, the decadal component of PDO is associated with below-normal monsoon mostly over west central part of India (Fig. 3a) compared to the total PDO index which suppresses rainfall over most of the India (see Fig. 11a of Krishnamurthy and Krishnamurthy, 2014a).

The signatures of winds and moisture flow are found to be consistent with the rainfall anomalies. The regression of vertically integrated moisture flux on PDO-D time series indicates that the moisture flow over the subcontinent is restricted below 20°N and the moisture does not reach beyond 20°N over India (Fig. 3b). This is in accordance with Fig. 3a where the drought condition exists north of 20°N indicating a lack of moisture flow towards the continent. The moisture flux pattern in Fig. 3b also differs from the regression pattern associated with the total PDO index obtained by Krishnamurthy and Krishnamurthy (2014a) (see their Fig. 11b). In the case of total PDO index, there is no moisture flux in the peninsular region while there is an outflow over northern Central India consistent with the weakening of the mean monsoon. Figure 3c, which includes the regression pattern of the moisture flux over a larger region, shows that the meridional winds bringing the moisture from the west North Pacific extend up to the vicinity of the Indian monsoon region. These northerly winds oppose the winds bringing moisture into the land regions north of 20°N. This explains the reason for lack of flow of moisture over west central part of India beyond 20°N.

4 Decadal PDO-monsoon relation in CCSM4

The discussion in section 3 highlights the differences between the influence of the pure decadal component of the PDO on the monsoon and the influence of the total PDO (which includes decadal and interannual components) as found in the study by Krishnamurthy and Krishnamurthy (2014a). The EOF analysis used in the conventional definition of the PDO cannot extract the signal that can be attributed to the decadal component of PDO alone. In order to overcome this problem, the MSSA method (discussed in section 2.3) can be employed to isolate the decadal variability in the North Pacific Ocean and in the Indian monsoon region, as demonstrated in another previous study by Krishnamurthy and Krishnamurthy (2014b). The application of MSSA on the observed rainfall over India yielded three decadal scale oscillations. One of the oscillations was identified to be related to the decadal part of the PDO. The spatial structure of this PDO-related oscillation in rainfall (Fig. 1e of Krishnamurthy and Krishnamurthy, 2014b) is similar to the precipitation regression pattern in Fig. 3a (except with opposite sign because of the ambiguity of sign in the EOF pattern). Krishnamurthy and Krishnamurthy (2014b) also obtained the pure decadal PDO by applying MSSA on SST anomalies in the North Pacific Ocean (see their Figs. 5d and 5e). In order to further substantiate the above observational results, the existence of similar decadal modes in rainfall and SST related to PDO are now explored in the CTL simulation of CCSM4.

4.1 Model control simulation

The MSSA was applied on 5-year running mean of JJAS seasonal anomaly of precipitation in CTL of CCSM4 for the period 1850–2005 over the domain 60°E–95°E, 5°N–35°N covering the Indian monsoon region. This analysis yielded three pairs of oscillatory modes. The RCs of these oscillations were constructed and examined by performing an EOF analysis of the RCs. The RC of the first oscillation obtained from the MSSA eigenmodes 1 and 2 was found to be related to PDO. The EOF1 of this RC and the corresponding PC1 in the model are shown in Fig. 4. The EOF1 indicates drought condition over most of the Indian monsoon region (Fig. 4a) while the PC1 shows decadal scale variability (Fig. 4b). The power spectrum analysis of PC1 of the RC indicates a peak around 26 years, as shown in Fig. 5a. The EOF1 and PC1 of this oscillation in the model have reasonable correspondence to the pure decadal PDO in the observation. The regression of JJAS seasonal anomaly of the model SST on PC1 indicates negative SST anomalies in the central North Pacific surrounded by positive anomalies along the west coast of North America (Fig. 5b). The maximum of positive anomalies in the central equatorial Pacific is shifted further to the west compared to observations (Fig. 2a). This SST regression pattern is representative of pure decadal variability of the PDO (further evidence will be provided in the next section). Based on the time period of the RC and the SST regression pattern, we identify this decadal mode in rainfall to be associated with the PDO. The second and the third oscillatory modes are related to the decadal variability of the North Atlantic Ocean and are discussed in a separate study by Krishnamurthy and

Krishnamurthy (2016b).

In a similar way, the MSSA was also performed with 5-year running mean of monthly mean SST anomalies in the North Pacific region (120°E–120°W, 20°N–60°N) in the CCSM4 CTL simulation using a lag window of 840 months to extract the PDO mode. After identifying the oscillatory pair of eigenmodes corresponding to the PDO, the RC of the oscillation was constructed. The EOF1 and PC1 of the RC of this oscillatory mode are shown in Fig. 6. The EOF1 represents the peak phase of PDO mode with negative SST anomalies in the central North Pacific surrounded by the positive SST anomalies (Fig. 6a) while the PC1 exhibits decadal scale variability (Fig. 6b). The power spectrum analysis of PC1 of the PDO mode indicates a period centered at 31 years (Fig. 7). Thus, CCSM4 has been able to simulate the observed pure decadal component of the PDO reasonably well. We used larger lag window for the model and experimental simulations as the model simulation has larger sample size than observations and hence allows us to use a larger lag window. The larger lag window allows us to better resolve the oscillatory modes and gain more quantitative information from the dynamical system (Ghil et al. 2002). We tested the MSSA on model data with different lag windows, and the results do not show any sensitivity to the choice of the lag window.

To determine the relation of the SST decadal PDO with the rainfall over India in CTL, regressions of SST and precipitation on PC1 of the PDO are shown in Fig. 8. The regression patterns of SST and rainfall indicate that the warm PDO phase is related to drought condition over India (except for the positive anomalies over east central part of

India) consistent with the negative correlation between the PDO and monsoon. The model shows bias in SST structure with slight westward shift in the SST anomalies in the tropical Pacific compared to observations. Consistent with the bias in the SST shift, there are biases in the location of the corresponding Walker and Hadley circulation response, which is reflected in the westward shift of the negative rainfall anomalies in the western part of India relative to observations. The mechanism needs to be further verified with models which do not have biases in SST with accurate simulation of PDO-related spatial structure in the tropical Pacific.

4.2 Model experiment

In order to isolate the influence of the North Pacific decadal variability on the Indian monsoon rainfall, a regionally de-coupled experiment (EXP) is performed with climatological SST prescribed in the North Pacific basin (see section 2.2). The results from the EXP simulation are compared with the CTL simulation to demonstrate the possible role of the North Pacific Ocean on the Indian monsoon.

An MSSA of 5-year running mean of JJAS seasonal anomalies of the Indian monsoon rainfall in EXP was performed for the period 1850-2005 using a lag window of 70 years, similar to the analysis of CTL. An examination of the MSSA eigenmodes indicated the absence of any oscillatory eigenmodes in rainfall in the timescale of the PDO. This provides a supporting evidence for the earlier result with the observations and CTL showing the existence of the PDO mode in the Indian monsoon rainfall on decadal

timescale.

The influence of the PDO on the Indian monsoon rainfall variability is further shown through the variance analysis of rainfall in the CTL and EXP simulations. It is well known that PDO exhibits broadband spectrum with a period of 20-40 years (e.g., Mantua and Hare 2002, Mantua et al. 1997). Our results suggest that the PDO-related modes in the rainfall and SST also show power spectrum with a period centered on the broadband between 20-40 years. Based on this inference, we used 20-40 year band pass filter on rainfall to evaluate the effect of PDO in the control and EXP simulations. The JJAS seasonal anomaly of rainfall was band-pass filtered in the 20-40 year band for both the CTL and EXP simulations. The variances of the filtered anomalies and the total anomalies were calculated for both the simulations. The ratio of the variance of the 20-40 year band-pass filtered anomalies to the variance of the total rainfall anomalies was determined, as shown in Fig. 9 for CTL and EXP simulations. There is reduced variance in rainfall over the central and southern parts of the Indian monsoon region and surrounding oceanic regions in the EXP simulation (Fig. 9b) relative to CTL simulation (Fig. 9a). The model has bias in simulating the rainfall over Himalayan region and hence it is not included in the interpretation of results. The reduction in the variability of the Indian monsoon rainfall in the PDO frequency band suggests that the North Pacific Ocean has considerable influence on the variability of rainfall over India on decadal timescale.

5 Role of the tropical Pacific

In an earlier study, Krishnamurthy and Krishnamurthy (2014a) suggested that the mechanism for the influence of PDO on monsoon involves the intermediary link through the tropical Pacific Ocean. The decadal variability associated with the tropical Pacific is compared here among the observations, control and experimental runs to further provide evidence for this mechanism. An MSSA of 5-year running mean of the observed monthly SST anomalies in the tropical Pacific domain (120°E–70°W, 30°S–30°N) results in an oscillatory pair of eigenmodes. The EOF1 and PC1 of the corresponding RC of the oscillation are shown in Figs. 10a and 10b, respectively. The EOF shows positive SST anomalies in the central and eastern Pacific surrounded by negative anomalies (Fig. 10a) while the PC indicates decadal variability (Fig. 10b). The power spectrum of PC1 (Fig. 11a) shows that this mode exhibits variability on the period of 27 years. The regression of monthly SST anomalies on PC1 results in a PDO-like pattern in the North Pacific Ocean with negative SST anomalies in the central North Pacific and positive SST anomalies extending from the west coast of North America to the tropical Pacific Ocean (Fig. 11b). Based on the period of oscillation and SST regression (Fig. 11), this decadal tropical mode is recognized to be related to the PDO and referred to as the equatorial PDO mode.

A similar MSSA was performed on the 5-year running mean of monthly SST anomalies from the CTL simulation over the tropical Pacific domain (120°E–70°W, 30°S–30°N). As in the case of observations, the MSSA of the SST anomalies in CTL also yields an oscillatory pair of eigenmodes. The EOF1 and PC1 of the RC of this oscillatory

mode (Figs. 12a, b) represent decadal scale variability in the tropical Pacific SST. The EOF pattern in the model (Fig. 12a) shows positive anomalies shifted westward compared to observation (Fig. 10a). Additionally, there is a region of negative anomalies in the eastern part. However, the model PC (Fig. 12b) indicates decadal variability, just as in the observation (Fig. 10b). The power spectrum of PC1 shows a peak centered at 32 years (Fig. 13a). The regression of model SST anomalies on PC1 of RC (Fig. 13b) also shows the PDO pattern in the North Pacific. This regression pattern (Fig. 13b) has close resemblance with the regression pattern shown earlier using the North Pacific PDO mode in CTL (Fig. 8a). Thus, the model CTL simulation also suggests the existence of the equatorial PDO mode similar to the observations.

The MSSA of the 5-year running mean of monthly SST anomalies in the tropical Pacific region (120°E–70°W, 30°S–30°N) was also repeated with the EXP simulation. The results showed the absence of equatorial PDO-like mode in the EXP simulation in contrast to observations and CTL simulation. These results suggest the influence of the PDO on the tropical Pacific Ocean, and support the possibility of PDO to affect the Indian monsoon through the tropical Pacific Ocean.

6 Summary and discussion

In this study, the relation between the pure decadal component of the PDO and the Indian monsoon has been examined. This work is extension of the study by

Krishnamurthy and Krishnamurthy (2014a) which explored the PDO-monsoon relation in observations and model control simulation. Krishnamurthy and Krishnamurthy (2014a) suggested negative correlation between the PDO and Indian monsoon with the warm (cold) phase of PDO related to drought (flood) conditions over Indian subcontinent. The mechanism for the PDO-monsoon relation was suggested through the Walker and Hadley circulations with the tropical Pacific playing an intermediary role between the North Pacific and Indian monsoon region. The conventional definition of PDO index was used to draw these conclusions. In the present study, the examination of the conventional PDO index has revealed that it includes both the interannual and decadal variability. Thus, the use of conventional PDO index may not represent the effect of the pure decadal component of PDO on the Indian monsoon. A pure decadal signal embedded in the PDO index was extracted by using SSA in this study. The influence of the pure decadal part of the PDO (also referred to as the decadal PDO for brevity) on the monsoon rainfall and winds was studied and compared with that of the total PDO which includes both interannual and decadal components. The total PDO index is associated with deficit monsoon rainfall over the entire subcontinent whereas the pure decadal part of PDO suppresses the monsoon mostly over west central part of India beyond 20°N and consistent with the restricted moisture flow beyond 20°N. This result distinguishes the effect of decadal PDO and total PDO and also suggests that the simple EOF analysis is inadequate to extract the pure decadal signal of the PDO.

An MSSA was performed on the rainfall anomalies over India and SST anomalies

over the North Pacific domain to obtain pure decadal signals in rainfall and SST. The observational results shown by Krishnamurthy and Krishnamurthy (2014b) document the PDO-related decadal modes in rainfall and SST and the relation between decadal IMR and decadal PDO variability. A similar analysis was performed in the present study with the CTL simulation (20C3M) to evaluate the ability of CCSM4 to represent the PDO-related decadal modes. The model also has a decadal mode in the North Pacific SST which represents the pure decadal signal of PDO. The Indian monsoon rainfall in the model also exhibits decadal mode related to PDO. The model is able to simulate the relation between decadal IMR and decadal PDO modes reasonably well. Similar analysis was performed using 500 years of pre-industrial control run and yields consistent results.

Further, a regionally de-coupled experiment, in which the North Pacific Ocean was prescribed with climatological SST was performed to substantiate the observed and model results on decadal PDO-monsoon relation. The EXP simulation shows the absence of decadal modes in the Indian monsoon rainfall on PDO timescale and supports the relation of PDO with the Indian monsoon variability. Further, the plausibility of the tropical Pacific playing an intermediary role in the relation between the PDO and Indian monsoon was explored by comparing the decadal variability in the tropical Pacific among observations, model control and experimental simulations. The tropical Pacific SST in the observations and CTL showed decadal mode of variability related to the PDO. However, the EXP did not reveal such a decadal mode, suggesting the plausibility of the mechanistic hypothesis proposed in Krishnamurthy and Krishnamurthy (2014a).

A residual PDO was also determined by subtracting the decadal PDO index from the conventional total PDO index (which has both decadal and interannual variability). The regressions of SST, rainfall, wind and moisture flux on the residual PDO (has interannual variability alone by construction) were examined (figures not shown). These regressions look similar to those of the conventional total PDO index, suggesting that the conventional PDO index predominantly represents the interannual variability of the North Pacific Ocean. Thus, this study has demonstrated the importance of determining the pure decadal component of the North Pacific Ocean to understand its effect on the Indian monsoon on decadal timescale. This study has investigated the influence of pure decadal PDO on Indian monsoon in model simulation and substantiated the observed and model simulated decadal relation between the PDO and monsoon through the regionally de-coupled experiments. Although the model simulation and experiment served as useful tools to substantiate the observed results, the model has some limitations such as bias in the rainfall over the Himalayan region, westward shift in the tropical Pacific SST anomalies related to PDO and slightly higher period of PDO compared to observations.

The results of this study have implications in understanding the effect of the decadal variability of oceans on the Indian monsoon on interannual to decadal timescales. The relative phases of the interannual PDO and decadal PDO determine the enhancement or suppression of the Indian monsoon. For example, if the interannual PDO is in warm phase, it suppresses the monsoon over entire India. Depending on the phase of decadal PDO, the west central India experiences normal monsoon (if decadal PDO is in cold

phase) or drought (if decadal PDO is in warm phase). Thus, this study will also provide insights on how the decadal modes of variability may modulate the interannual variability of the monsoon rainfall. The information on the relation between the decadal signals in rainfall and SST may also help in advancing the decadal prediction which is still in its infancy.

Acknowledgments

This work was supported by National Science Foundation (grants 0830062 and 0830068), National Oceanic and Atmospheric Administration (grant NA09OAR4310058), and National Aeronautics and Space Administration (grant NNX09AN50G). The authors thank NCAR for providing the data of 20C3M simulation, computational time and technical help with model experiments. We also thank the anonymous reviewers for helpful comments which have helped improve the manuscript. This work formed a part of the Ph.D. thesis of Lakshmi Krishnamurthy at George Mason University.

References

Allen MR, Robertson AW. 1996. Distinguishing modulated oscillations from coloured noise in multivariate datasets. *Clim Dyn* **12**:775–784

Allen MR, Smith LA 1996. Monte Carlo SSA: Detecting irregular oscillations in the presence of colored noise. *J Clim* **9**:3373–3404

Broomhead, DS, King GP 1986. Extracting qualitative dynamics from experimental data. *Physica D* **20**: 217–236

Compo GP et al 2011. The twentieth century reanalysis project. *Quart J Roy Meteor Soc* **137**: 1–28

Dominguez, F, Kumar P 2005. Dominant modes of moisture flux anomalies over North America. *J. Hydrometeor* **6:** 194–209.

Gent PR et al 2011. The Community Climate System Model Version 4. *J Clim* **24**: 4973–4991

Ghil M et al 2002. Advanced spectral methods for climatic time series. *Rev Geophys* **40(1):**1003. doi:200210.1029/2000RG000092

Huang B 2004. Remotely forced variability in the tropical Atlantic Ocean. *Clim Dyn* **23**:133–152

Huang B, Schopf PS, Shukla J 2004. Intrinsic Ocean–Atmosphere Variability of the Tropical Atlantic Ocean. *J Clim* **17**:2058–2077

Leith CE 1973. The Standard Error of Time-Average Estimates of Climatic Means. *J. Appl. Meteor* **12**: 1066–1069.

Krishnan R, Sugi M 2003. Pacific decadal oscillation and variability of the Indian summer monsoon rainfall. *Clim Dyn* **21**: 233–242

Krishnamurthy L, Krishnamurthy V 2014a. Influence of PDO on South Asian summer monsoon and monsoon–ENSO relation. *Clim Dyn* **42**:2397–2410

Krishnamurthy L, Krishnamurthy V 2014b. Decadal scale oscillations and trend in the Indian monsoon rainfall. *Clim Dyn* **43**:319–331

Krishnamurthy L, Krishnamurthy V 2016a. Decadal and interannual variability of the Indian Ocean SST. *Clim Dyn*. **46**:57–70

Krishnamurthy L, Krishnamurthy V 2016b. Teleconnections of Indian monsoon rainfall with AMO and Atlantic tripole. *Clim Dyn* **46**:2269–2285

Krishnamurthy V, Goswami BN 2000. Indian monsoon–ENSO relationship on interdecadal timescale. *J Clim* **13**: 579–595

Li S, Perlwitz J, Quan X, Hoerling MP 2008. Modelling the influence of North Atlantic multidecadal warmth on the Indian summer rainfall. *Geophys Res Lett* **35**:L05804. doi:200810.1029/2007GL032901

Lu R, Dong B, Ding H 2006. Impact of the Atlantic Multidecadal Oscillation on the Asian summer monsoon. *Geophys Res Lett* **33**:L24701. doi:10.1029/2006GL027655

Mantua NJ, Hare SR, Zhang Y, Wallace JM, Francis RCA 1997. Pacific interdecadal climate oscillation with impacts on salmon production. *Bull Amer Meteor Soc* **78**:1069–1079

Plaut G, Vautard R 1994. Spells of Low-Frequency Oscillations and Weather Regimes in the Northern Hemisphere. *J. Atmos. Sci* **51**: 210–236

Rasmusson EM, Carpenter TH 1983. The relationship between eastern equatorial Pacific sea surface temperatures and rainfall over India and Sri Lanka. *Mon Wea Rev* **111**: 517–528

Rajeevan M, Bhate J, Kale J, Lal B 2006. High resolution daily gridded rainfall data for the Indian region: Analysis of break and active monsoon spells. *Curr Sci* **91**:296–306

Rayner NA, Parker DE, Horton EB, Folland CK, Alexander LV, Rowell DP, Kent EC, Kaplan A 2003. Global analyses of sea surface temperature, sea ice, and night marine air temperature since the late nineteenth century. *J Geophys Res* **108**(D14):4407. doi:10.1029/2002J0002670

Sen Roy S 2011. Identification of periodicity in the relationship between PDO, El Niño and peak monsoon rainfall in India using S-transform analysis. *Int J Climatol*. **31**: 1507–1517

Sen Roy S, Goodrich GB, Balling RC 2003. Influence of El Niño/southern oscillation, Pacific decadal oscillation, and local sea-surface temperature anomalies on peak season monsoon precipitation in India. *Clim Res* **25**: 171–178

Sikka DR 1980. Some aspects of the large scale fluctuations of summer monsoon rainfall over India in relation to fluctuations in the planetary and regional scale circulation parameters. *Proc Indian Natl Acad Sci* **89**: 179–195

Smith RD et al 2010. The Parallel Ocean Program (POP) reference manual. *Los Alamos National Laboratory Tech Rep*, LAUR-10-01853, pp 1–140

Turner AG, Annamalai H 2012. Climate change and the South Asian summer monsoon. *Nature Climate Change*, **2**:587-595

Zhang R, Delworth TL 2006. Impact of Atlantic multidecadal oscillations on India/Sahel rainfall and Atlantic hurricanes. *Geophys Res Lett*, **33**:L17712. doi:10.1029/2006GL026267

Figure Captions

Figure 1 (a) Conventional PDO index: PC1 obtained by EOF analysis of monthly SST anomalies over (120°E–120°W, 20°N–60°N) for the period 1870–2006. (b) Decadal PDO (PDO-D) index: Monthly RC time series obtained by applying SSA on monthly conventional PDO index (shown in a). (c) Power spectra of RC time series shown in (b). The peak of the power spectra is above the corresponding red noise spectrum (dashed) at 5% significance level.

Figure 2 Regression of JJAS seasonal anomaly of (a) SST (b) Smith et al. (2010) rainfall on PDO-D index shown in Fig. 1b. The dotted regions indicate values above 5% significance level. The units are in °C for SST and mm day^{-1} for rainfall per standard deviation of corresponding time series.

Figure 3 Regression of JJAS seasonal anomaly of (a) IMD rainfall (b) vertically integrated stationary moisture flux on rainfall on PDO-D index shown in Fig. 1b. (c) is same as (b) except that it is shown only over a larger region. The units are in mm day^{-1} for rainfall and Kg m s^{-1} for the moisture flux per standard deviation of corresponding time series. The dotted regions in (a) and grey shaded regions in (b), (c) indicate values above 5% significance level.

Figure 4 (a) EOF1 and (b) PC1 of RC of the first oscillatory pair of precipitation over the Indian monsoon region in the model CTL simulation.

Figure 5 (a) Power spectrum of PC1 of RC of CTL shown in Fig. 4b. The peak of the power spectra is above the corresponding red noise spectrum (dashed) at 5%

significance level. (b) Regression of SST on PC1 of RC shown in Fig. 4b. The dotted regions indicate values above 5% significance level. The units are in °C per standard deviation of corresponding time series.

Figure 6 (a) EOF1 and (b) PC1 of the RC of the decadal mode in SST over the North Pacific domain (120°E–120°W, 20°N–60°N) in the model CTL simulation.

Figure 7 Power spectrum of PC1 of RC of CTL shown in Fig. 6b. The peak of the power spectra is above the corresponding red noise spectrum (dashed) at 5% significance level.

Figure 8 Regression of JJAS seasonal anomalies of (a) SST and (b) rainfall on PC1 of RC in CTL shown in Fig. 6b. The dotted regions indicate values above 5% significance level. The units are in °C for SST and mm day^{-1} for rainfall per standard deviation of corresponding time series.

Figure 9 Ratio of the variance of 20-40 band-pass filtered anomalies to the variance of the total anomalies of precipitation in the model (a) CTL and (b) EXP simulations.

Figure 10 (a) EOF1 and (b) PC1 of the RC of the decadal mode in SST over the tropical Pacific domain (120°E–120°W, 30°S–30°N) in observation.

Figure 11 (a) Power spectrum of PC1 of RC of observation shown in Fig. 10b. The peak of the power spectra is above the corresponding red noise spectrum (dashed) at 5% significance level. (b) Regression of observed SST anomalies on PC1 of RC shown in Fig. 10b. The dotted regions indicate values above 5% significance level. The units are in

°C per standard deviation of corresponding time series.

Figure 12 (a) EOF1 and (b) PC1 of the RC of the decadal mode in SST over the tropical Pacific domain (120°E–120°W, 30°S–30°N) in model CTL simulation.

Figure 13 (a) Power spectrum of PC1 of RC of the model CTL simulation shown in Fig. 12b. The peak of the power spectra is above the corresponding red noise spectrum (dashed) at 5% significance level. (b) Regression of CTL SST anomalies on PC1 of RC shown in Fig. 12b. The dotted regions indicate values above 5% significance level. The units are in K per standard deviation of corresponding time series.

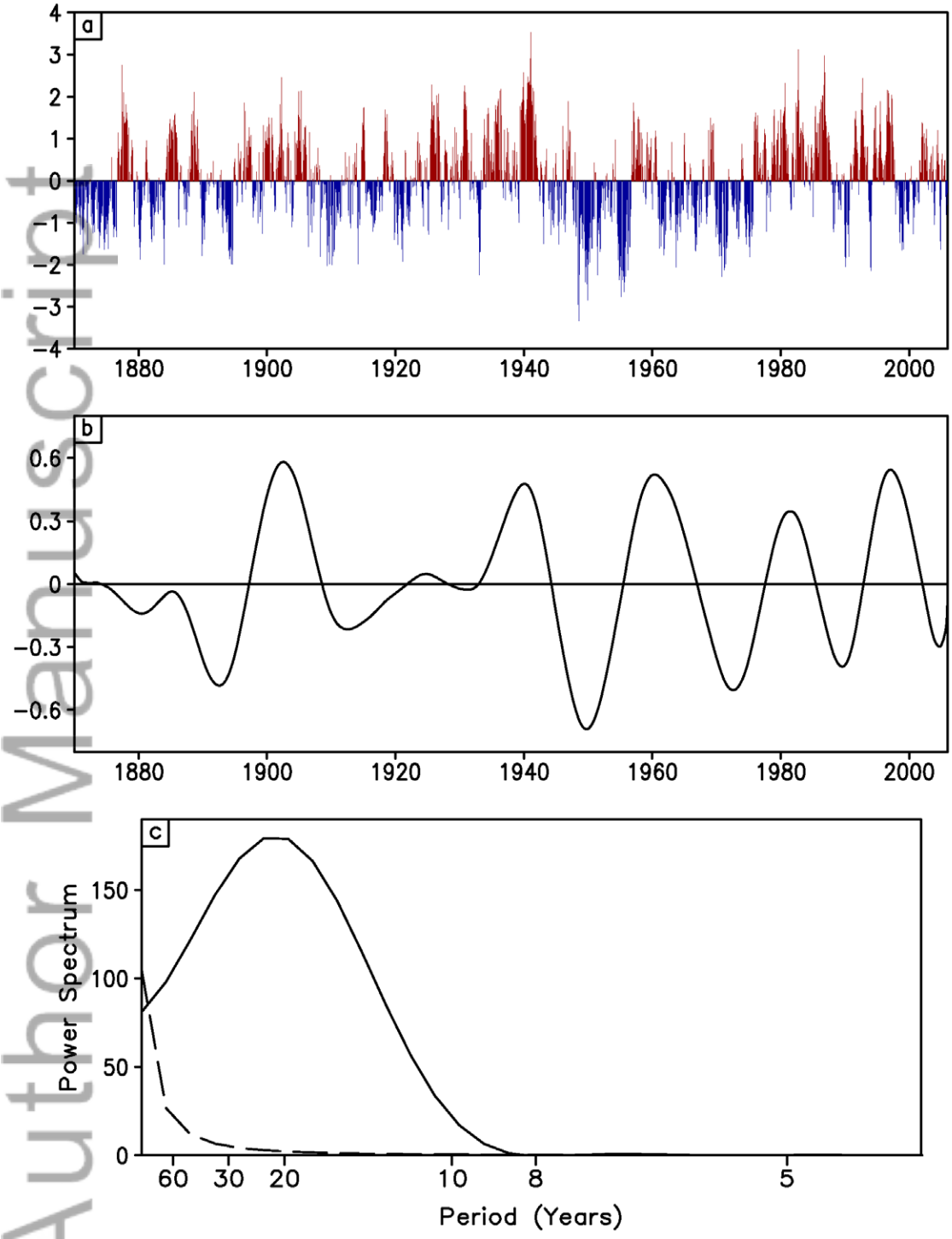

Figure 1 (a) Conventional PDO index: PC1 obtained by EOF analysis of monthly SST anomalies over (120°E–120°W, 20°N–60°N) for the period 1870–2006. (b) Decadal PDO (PDO-D) index: Monthly RC time series obtained by applying SSA on monthly conventional PDO index (shown in a). (c) Power spectra of RC time series shown in (b). The peak of the power spectra is above the corresponding red noise spectrum (dashed) at 5% significance level.

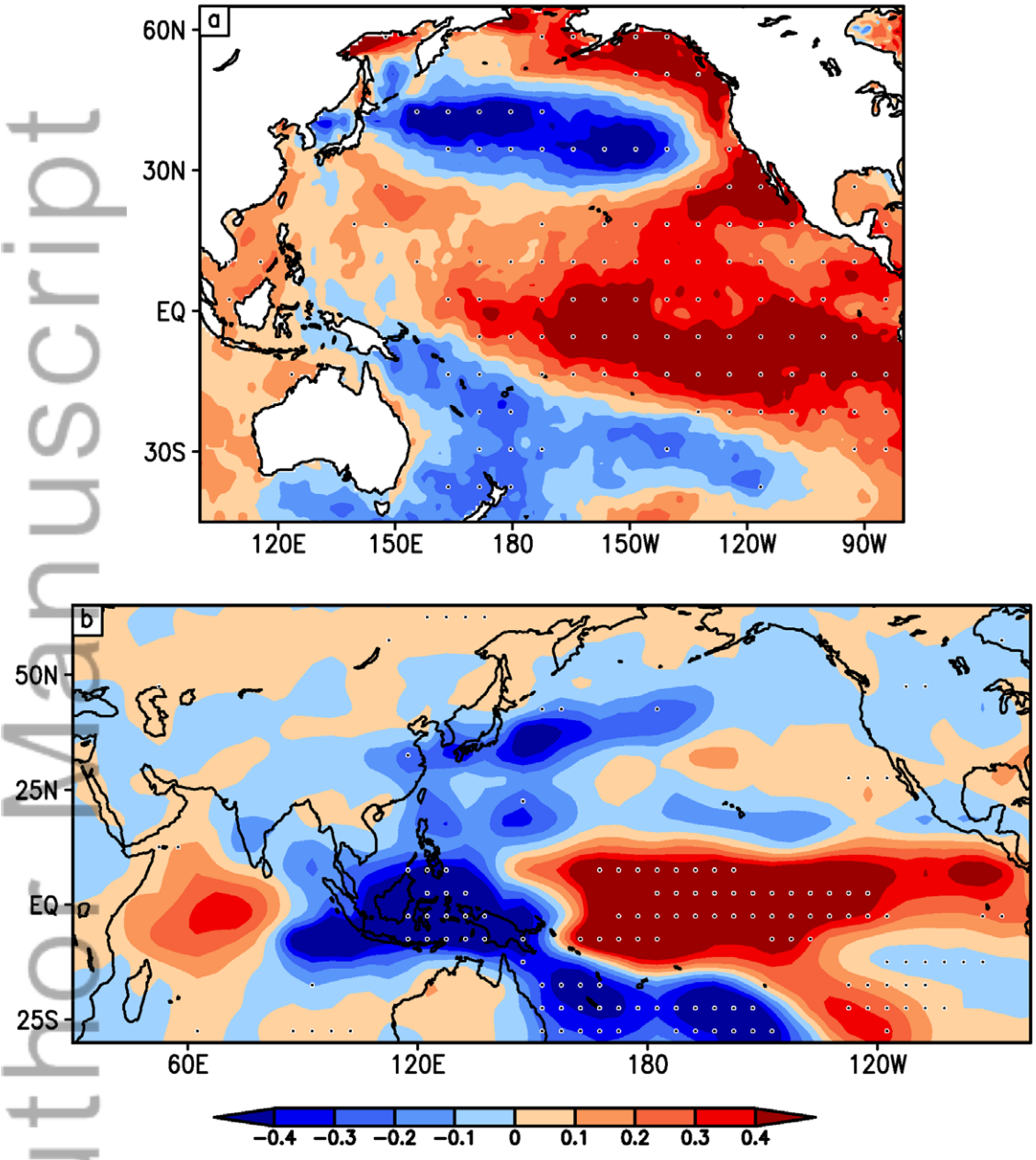

Figure 2 Regression of JJAS seasonal anomaly of (a) SST (b) Smith et al. (2010) rainfall on PDO-D index shown in Fig. 1b. The dotted regions indicate values above 5%

significance level. The units are in °C for SST and mm day^{-1} for rainfall per standard deviation of corresponding time series.

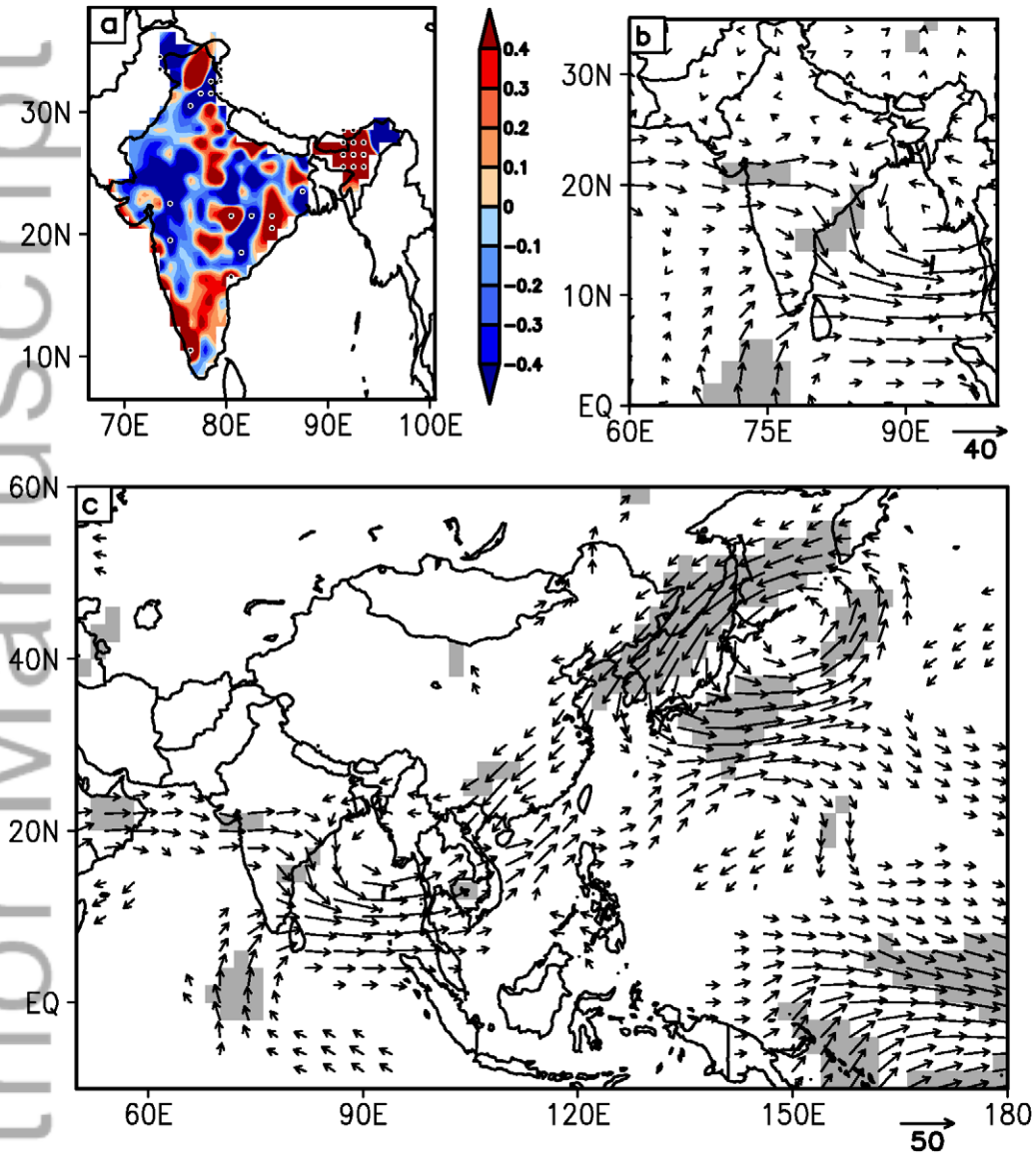

Figure 3 Regression of JJAS seasonal anomaly of (a) IMD rainfall (b) vertically

integrated stationary moisture flux on rainfall on PDO-D index shown in Fig. 1b. (c) is same as (b) except that it is shown only over a larger region. The units are in mm day^{-1} for rainfall and Kg m s^{-1} for the moisture flux per standard deviation of corresponding time series. The dotted regions in (a) and grey shaded regions in (b), (c) indicate values above 5% significance level.

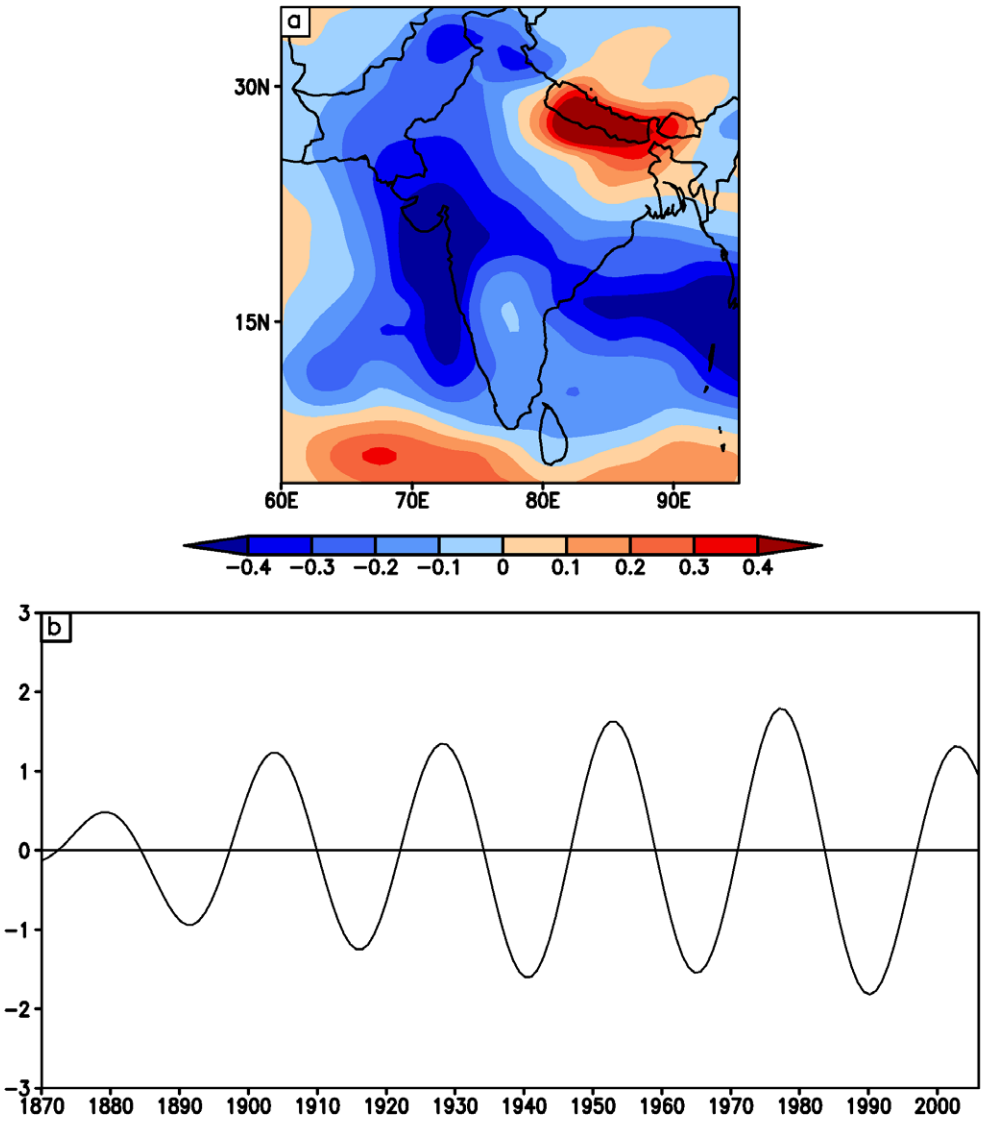

Figure 4 (a) EOF1 and (b) PC1 of RC of the first oscillatory pair of precipitation over the Indian monsoon region in the model CTL simulation.

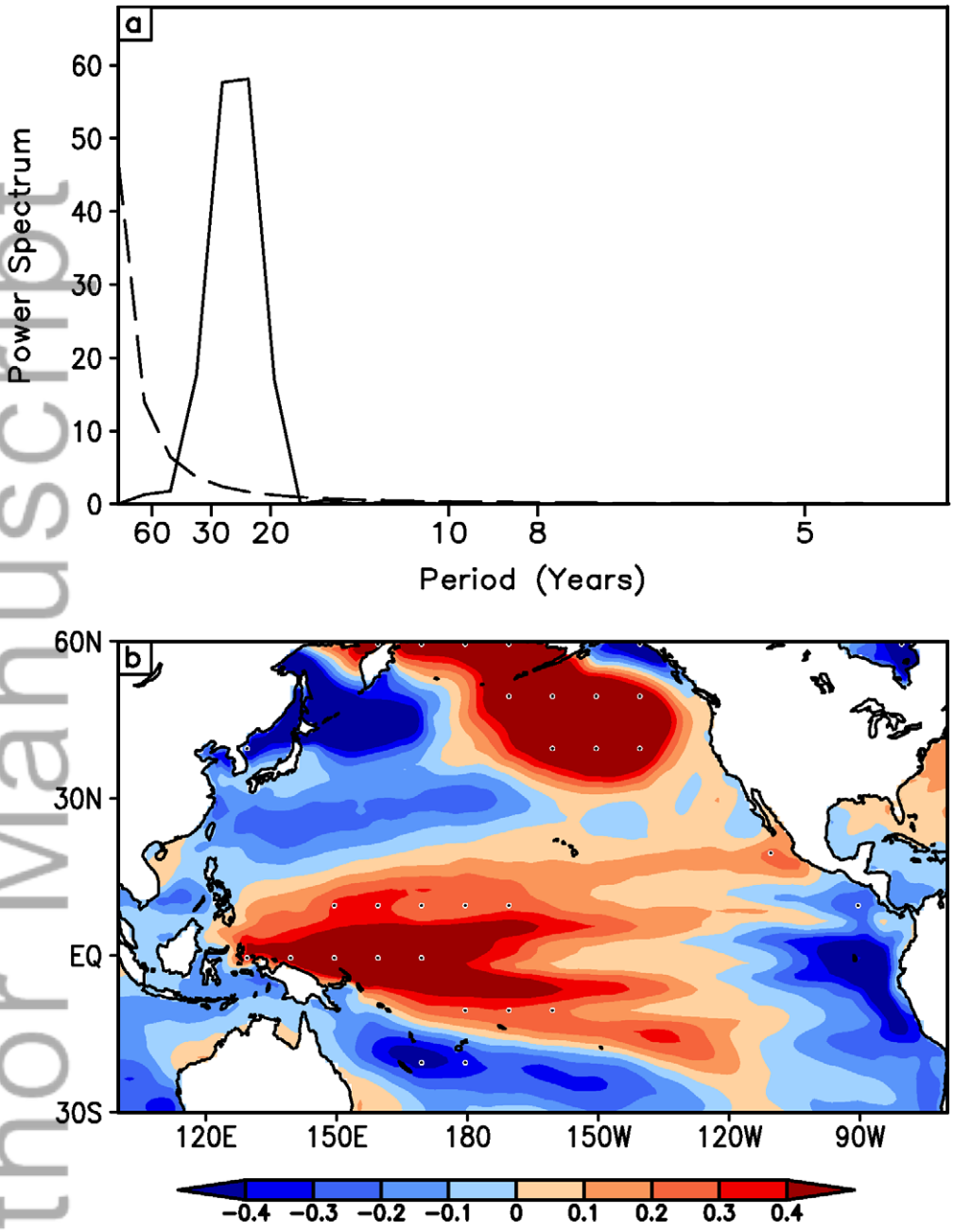

Figure 5 (a) Power spectrum of PC1 of RC of CTL shown in Fig. 4b. The peak of the power spectra is above the corresponding red noise spectrum (dashed) at 5% significance

level. (b) Regression of SST on PC1 of RC shown in Fig. 4b. The dotted regions indicate values above 5% significance level. The units are in °C per standard deviation of corresponding time series.

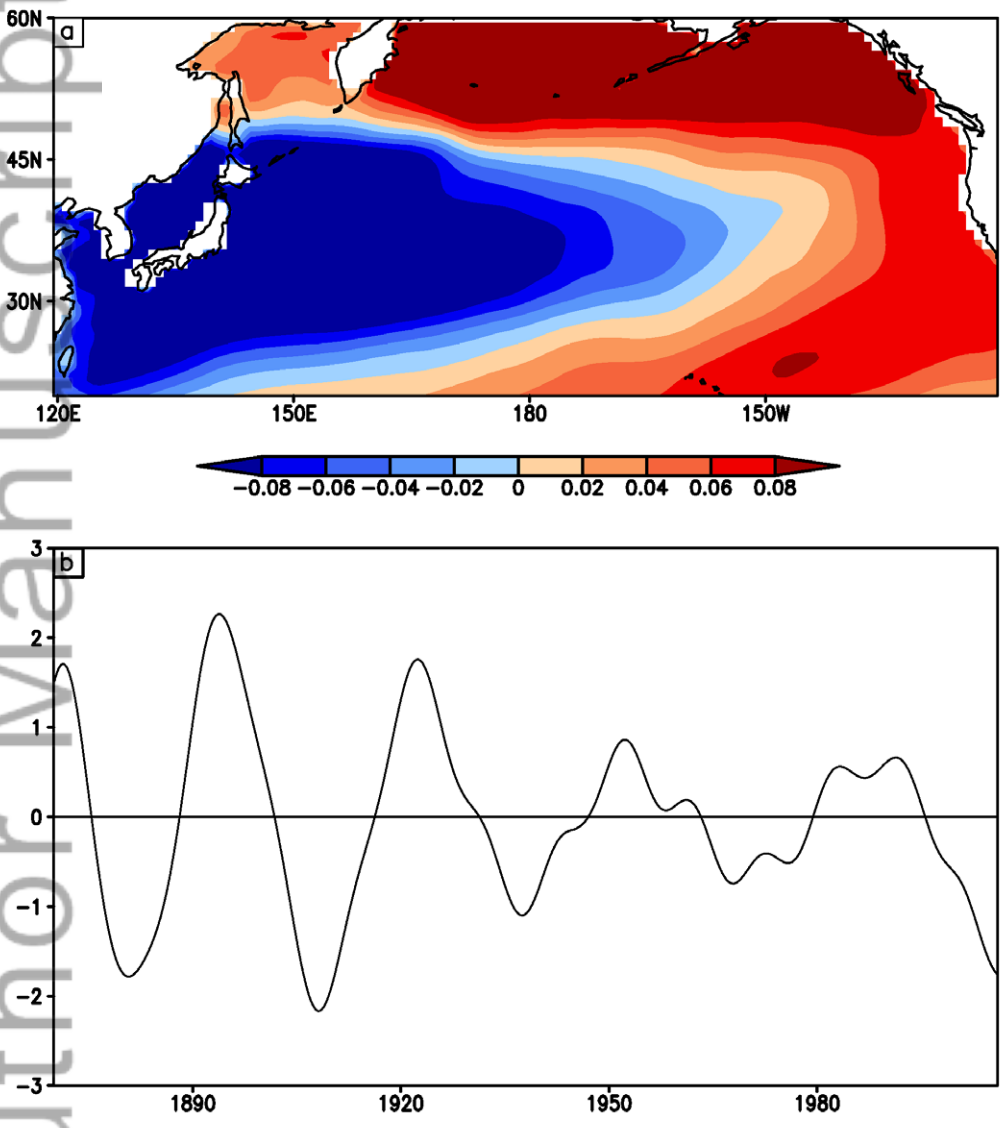

Figure 6 (a) EOF1 and (b) PC1 of the RC of the decadal mode in SST over the North Pacific domain (120°E–120°W, 20°N–60°N) in the model CTL simulation.

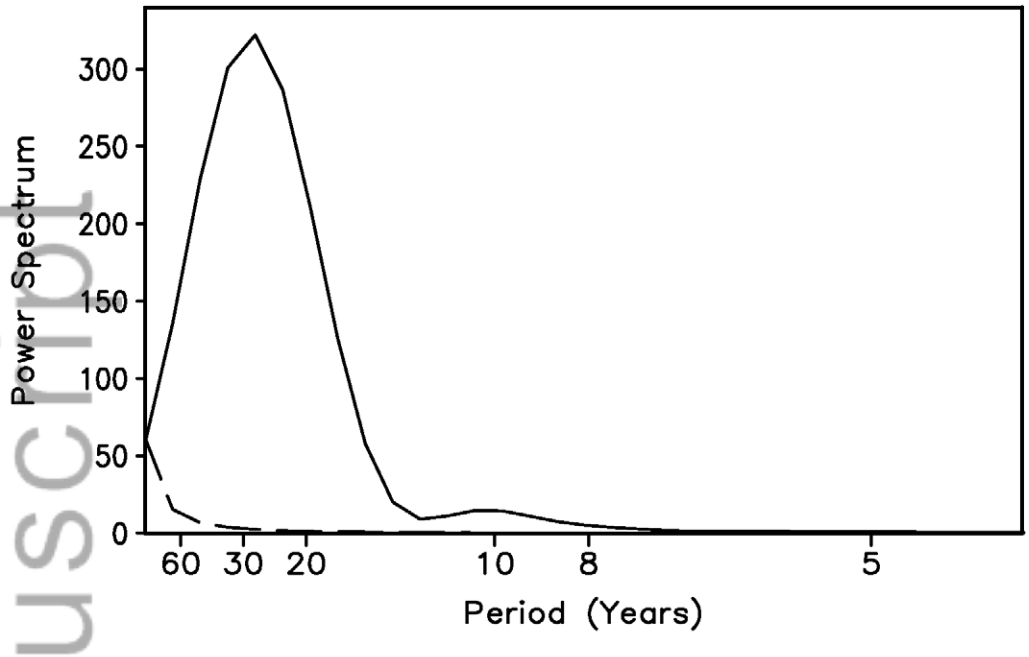

Figure 7 Power spectrum of PC1 of RC of CTL shown in Fig. 6b. The peak of the power spectra is above the corresponding red noise spectrum (dashed) at 5% significance level.

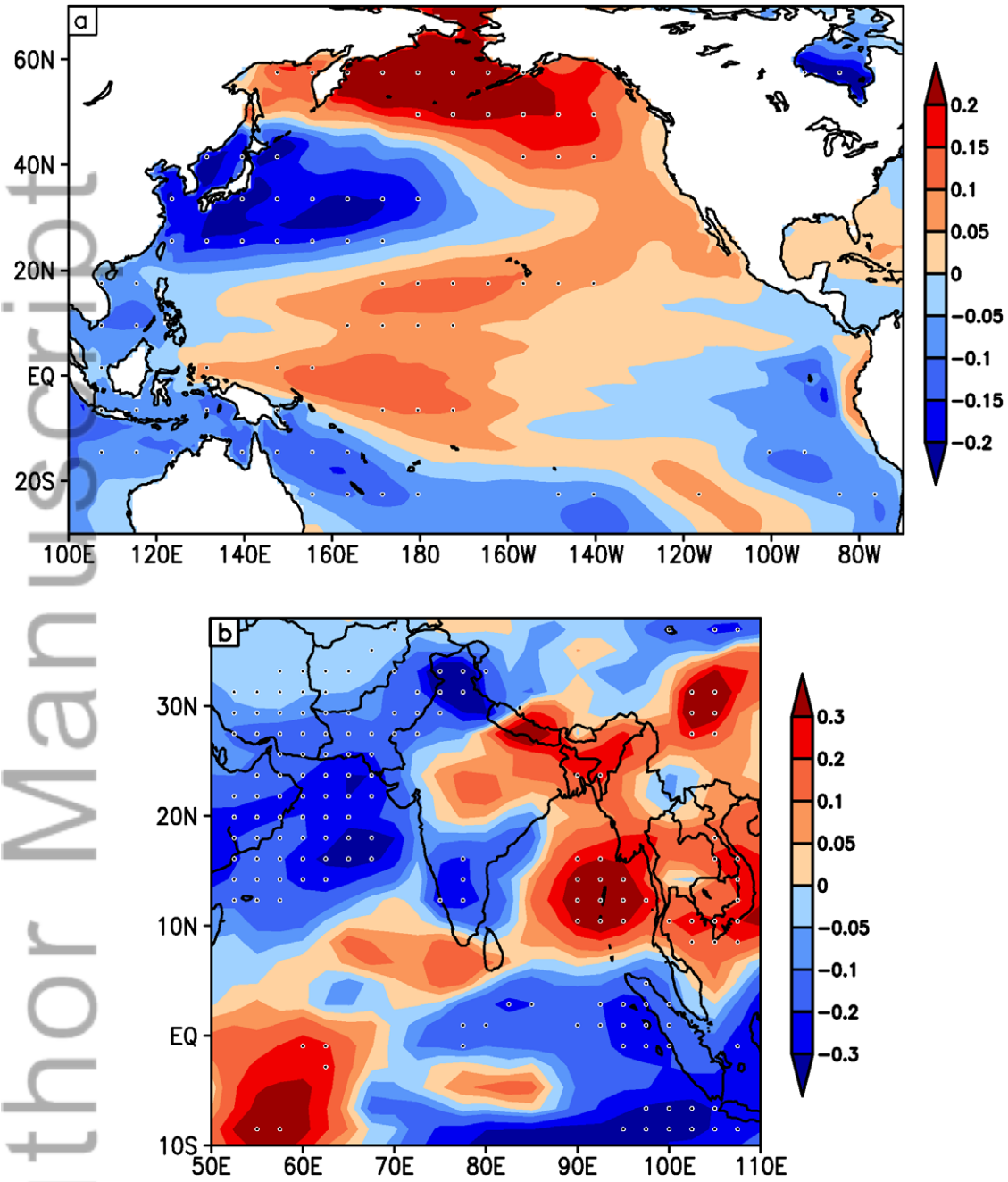

Figure 8 Regression of JJAS seasonal anomalies of (a) SST and (b) rainfall on PC1 of RC in CTL shown in Fig. 6b. The dotted regions indicate values above 5% significance level.

The units are in °C for SST and mm day^{-1} for rainfall per standard deviation of corresponding time series.

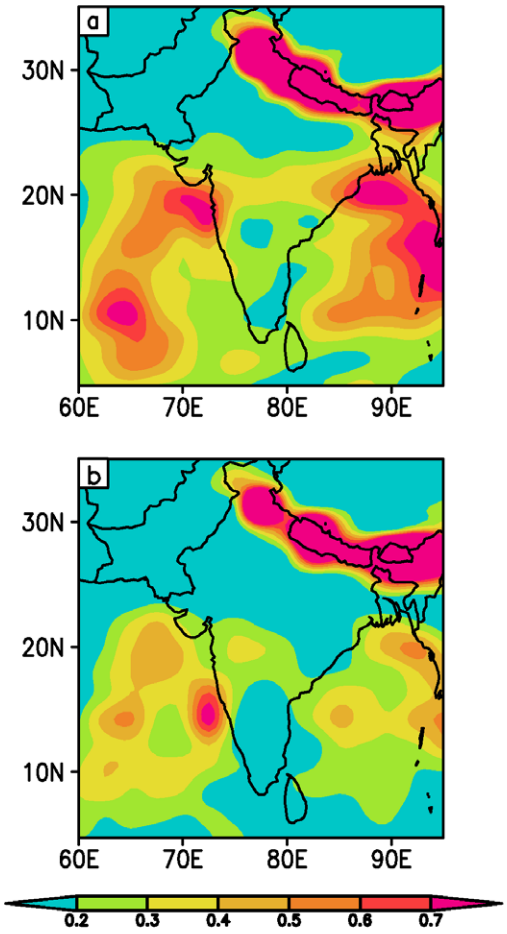

Figure 9 Ratio of the variance of 20-40 band-pass filtered anomalies to the variance of the total anomalies of precipitation in the model (a) CTL and (b) EXP simulations.

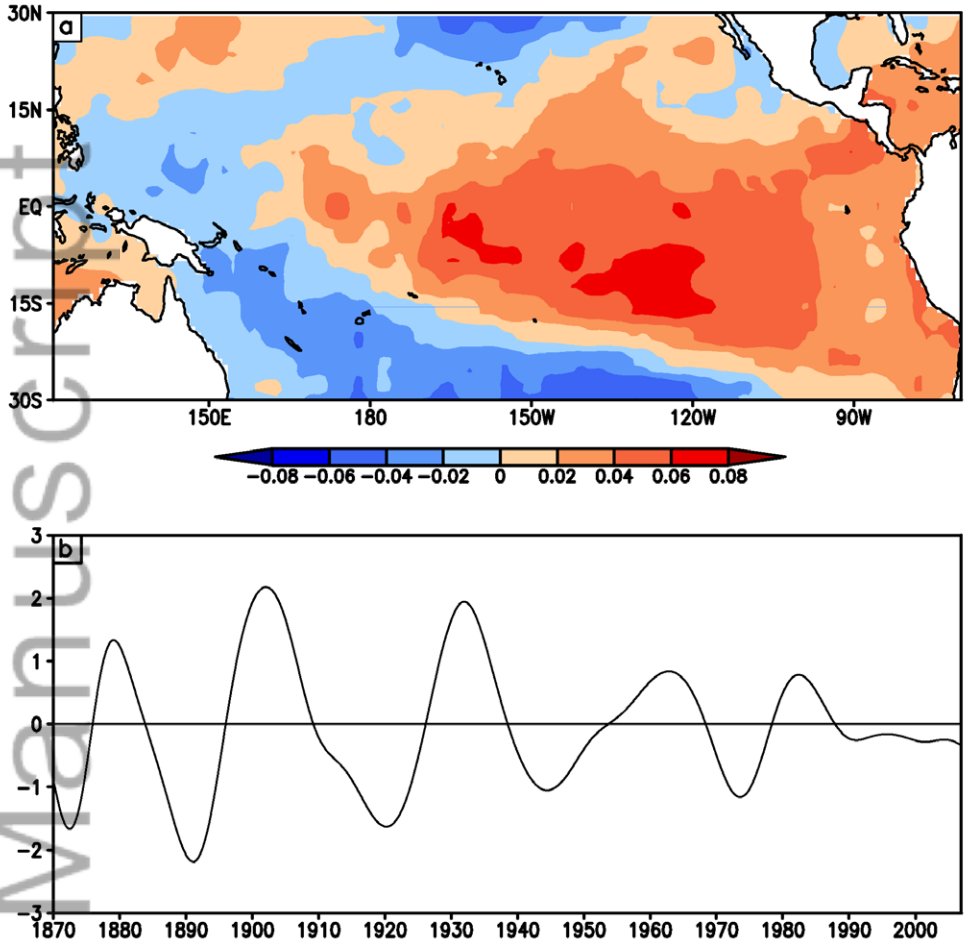

Figure 10 (a) EOF1 and (b) PC1 of the RC of the decadal mode in SST over the tropical Pacific domain (120°E–120°W, 30°S–30°N) in observation.

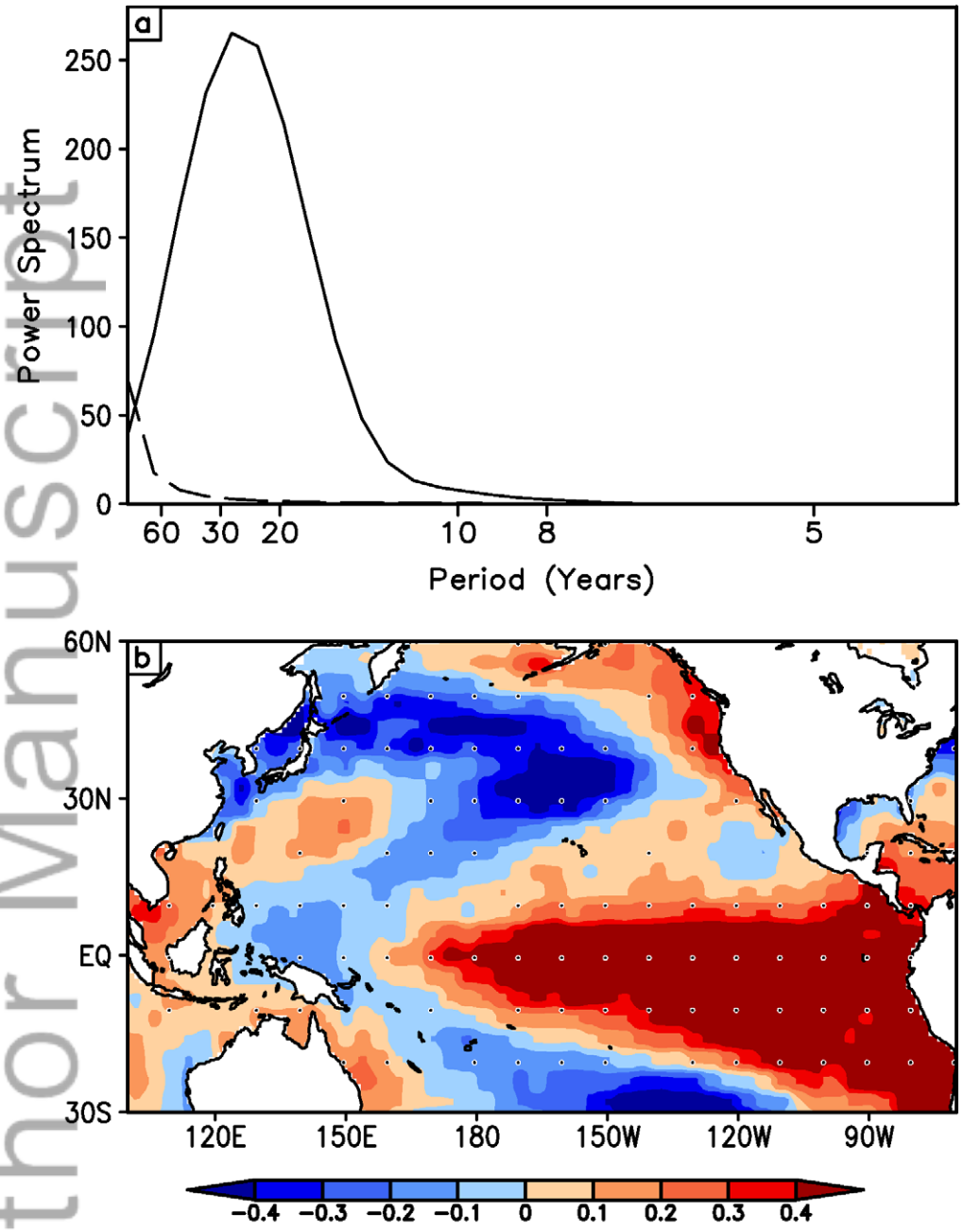

Figure 11 (a) Power spectrum of PC1 of RC of observation shown in Fig. 10b. The peak of the power spectra is above the corresponding red noise spectrum (dashed) at 5%

significance level. (b) Regression of observed SST anomalies on PC1 of RC shown in Fig. 10b. The units are in °C per standard deviation of corresponding time series.

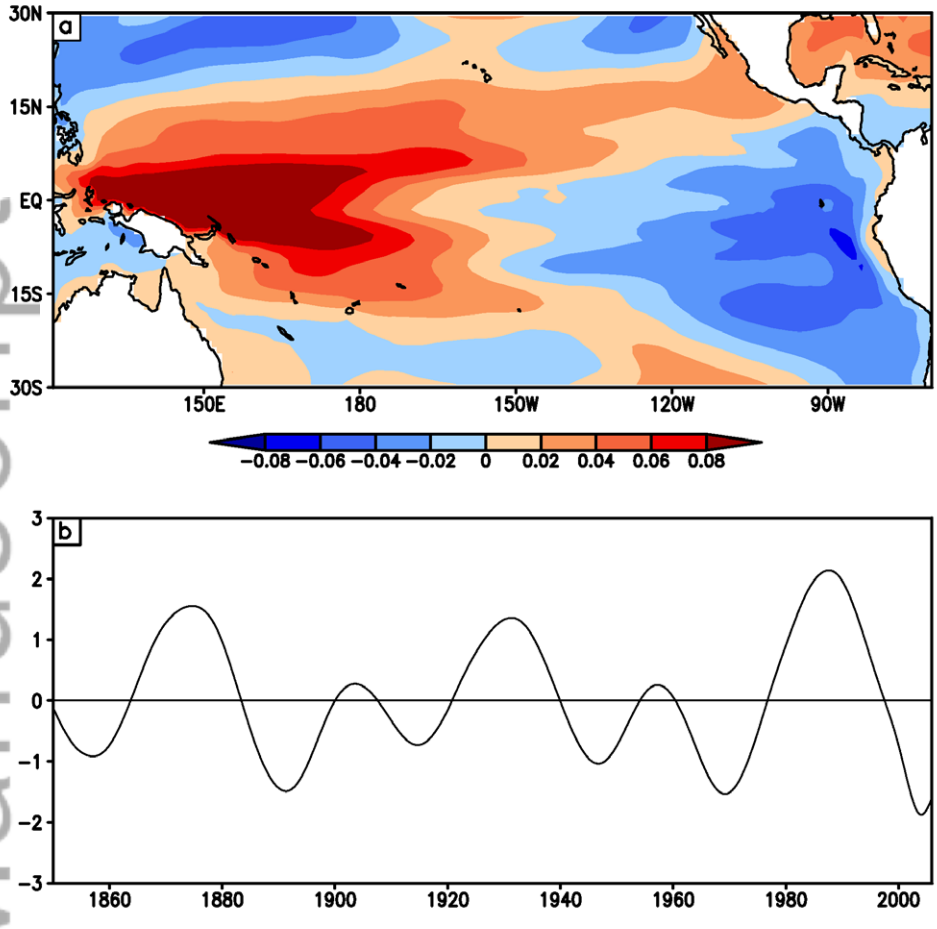

Figure 12 (a) EOF1 and (b) PC1 of the RC of the decadal mode in SST over the tropical Pacific domain (120°E–120°W, 30°S–30°N) in model CTL simulation.

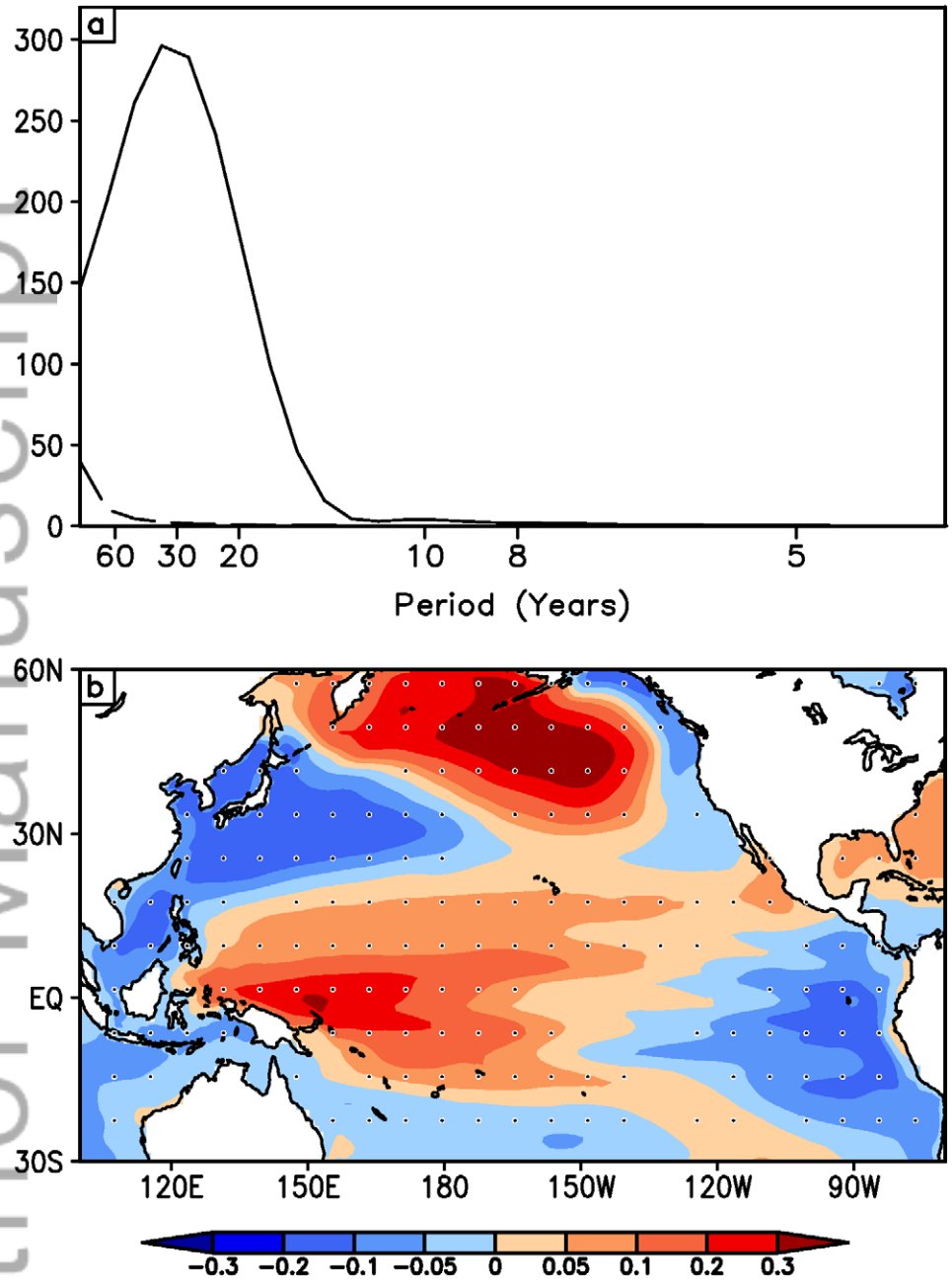

Figure 13 (a) Power spectrum of PC1 of RC of the model CTL simulation shown in Fig. 12b. The peak of the power spectra is above the corresponding red noise spectrum (dashed) at 5% significance level. (b) Regression of CTL SST anomalies on PC1 of RC shown in Fig. 12b. The dotted regions indicate values above 5% significance level. The units are in °C per standard deviation of corresponding time series.